© [2009] IEEE. Reprinted, with permission, from Wang, Yi., Zhang., Zhu, Jianguo., Yongchang., Guo, Youguang., Yongjian, Li., Xu, Wei., & Ertugrul, N. Initial Rotor Position and Magnet Polarity Identification of PM Synchronous Machines Based on Numerical Simulation. Proceedings of 19th Australasian Universities Power Engineering Conference. This material is posted here with permission of the IEEE. Such permission of the IEEE does not in any way imply IEEE endorsement of any of the University of Technology, Sydney's products or services. Internal or personal use of this material is permitted. However, permission to reprint/republish this material for advertising or promotional purposes or for creating new collective works for resale or redistribution must be obtained from the IEEE by writing to pubs-permissions@ieee.org. By choosing to view this document, you agree to all provisions of the copyright laws protecting it.

Initial Rotor Position and Magnet Polarity Identification of PM Synchronous Machines Based on Numerical Simulation

Yi Wang, Jianguo Zhu, Youguang Guo, Yongjian Li, and Wei Xu
School of Electrical, Mechanical and Mechatronic Systems
University of Technology, Sydney
Sydney, Australia

***Abstract*—In this paper a comprehensive nonlinear model of surface mounted permanent magnet (PM) synchronous machine (SPMSM) is developed considering both the structural and saturation saliencies. After experimentally identifying all the parameters, a nonlinear mathematic model of SPMSM is built, in which the rotor position and stator current are taken as the variables to calculate the inductances. A pulse injection based scheme is proposed to detect the initial rotor position and magnet polarity. A rotor vibration analysis is carried out to finalize the injected signal. The saturation saliency embedded in the nonlinear model is utilized to identify the rotor polarity, which is essential for starting the SPMSM. Simulations are taken for several different rotor initial positions and the result shows that the proposed method is suitable for the SPMSM drive.**

Keywords-initial rotor position; nonlinear magnetic model; PM synchronous machines; saturation saliency; structual saliency.

I. INTRODUCTION

Permanent magnet (PM) machines, such as permanent magnet synchronous machines (PMSMs), have found wide applications due to their high power density (compactness), high efficiency, ease of control, high torque-to-inertia ratio, and high reliability. However, a rotor position sensor is often required in a PMSM drive system, which will not only increase the system cost, but also perhaps more importantly reduce the system reliability [1]. Even for some instinctive sensorless drive methods such as the direct torque control (DTC), the initial rotor position detection is unavoidable [2].

A number of signal injection techniques for position sensorless and initial rotor position detection have been proposed based on tracking the rotor magnetic saliency [3] [4]. The magnetic saliencies inside a PMSM can be classified as the structural saliency that mainly comes from the interior structure, and the saturation saliency induced by the magnetic saturation effect of the stator core. The saturation saliency has to be utilized for identifying the rotor polarity for both the interior PMSM (IPMSM) and surface mounted PMSM (SPMSM).

The experimental trial and error method has to be employed because the conventional PMSM model does not incorporate the saturation saliency [5]. When developing a new method for the rotor position detection, it is not possible to numerically simulate the proposed scheme.

In [6], a DC pulse injection method was proposed and implemented, but the rotor vibration during the signal injection was not discussed. A numerical simulation was carried out by Yan *et al.* in [7]. However, the rotor position is fixed during the injection and the nonlinear model reported is only based on 5.5A current offset. It is not enough to analyze the current response in the stator windings.

In this paper, a comprehensive nonlinear mathematical model of SPMSM is built considering the magnetic saturation saliency. A numerical nonlinear inductance model is proposed based on the stator currents and rotor position variation with all the parameters experimentally identified. Based on the analytical solution, the rotor angle vibration is expressed as a response function of the injected signal. A series of DC voltage pulse are injected into the stator windings to determine the rotor initial position. To minimize the rotor vibration, the rotor axis position is detected firstly based on low magnitude pulse injection. Two high magnitude voltage pulses are injected later to detect the rotor polarity based on the stator core saturation. The nonlinear machine model and the proposed scheme are simulated in SIMULINK and the initial rotor position detection performance is evaluated at different initial rotor angles. The results show that the proposed scheme is suitable for SPMSM initial position and magnet polarity detection.

II. NONLINEAR MODEL OF SPMSM WITH SALIENCIES

A. Nonlinear SPMSM model

In an SPMSM, the observable total flux linkage λ_t inside the air-gap is contributed by both the stator currents and the permanent magnets on the rotor and it is the link between the stator and rotor magnetic fields. The three-phase flux linkages λ_{abc} are here defined as the projection of λ_t on the stator reference frame. The voltage equation of the stator windings can be written as

$$v_{abc} = R_s i_{abc} + \frac{d}{dt}\lambda_{abc} \tag{1}$$

where v_{abc}, i_{abc} and R_s are the phase voltages, currents and winding resistance in the stator reference frame, respectively.

The relationship between the current and flux linkage is usually described by a nonlinear magnetization curve. In the conventional linear PMSM model, this magnetization curve is assumed to be linear, and the linear PMSM model can be expressed as

$$v_{abc} = R_s i_{abc} + L_{abc} \frac{d}{dt} i_{abc} \tag{2}$$

where L_{abc} is the three-phase inductance matrix including the self- and mutual-inductances and it is independent of the stator currents. In the rotor reference frame, the d- and q-axis inductances are thereby constant. When a set of unequal d- and q-inductances are employed, the structural saliency of a PM machine can be calculated based on this model. However, this linear model cannot be used to describe the nonlinear saturation saliency.

For a nonlinear model, the magnetic saturation should be considered and the inductances are expressed as incremental inductances, which vary against the stator current. Then a composite function can be used to express the flux linkage as

$$\lambda_a = f(i_{abc}, \theta) \tag{3}$$

where θ is the rotor position angle.

The following differential equations can be obtained

$$\begin{bmatrix} v_a \\ v_b \\ v_c \end{bmatrix} = R_s \begin{bmatrix} i_a \\ i_b \\ i_c \end{bmatrix} + L^*_{abc} \frac{d}{dt} \begin{bmatrix} i_a \\ i_b \\ i_c \end{bmatrix} + \frac{\partial}{\partial \theta} \begin{bmatrix} \lambda_a \\ \lambda_b \\ \lambda_c \end{bmatrix} \omega_e \tag{4}$$

where $\frac{\partial}{\partial \theta} \begin{bmatrix} \lambda_a \\ \lambda_b \\ \lambda_c \end{bmatrix} \omega_e$ is the rotating back-emf in the three-phase windings;

$$L^*_{abc} = \begin{bmatrix} \frac{\partial \lambda_a}{\partial i_a} & \frac{\partial \lambda_a}{\partial i_b} & \frac{\partial \lambda_a}{\partial i_c} \\ \frac{\partial \lambda_b}{\partial i_a} & \frac{\partial \lambda_b}{\partial i_b} & \frac{\partial \lambda_b}{\partial i_c} \\ \frac{\partial \lambda_c}{\partial i_a} & \frac{\partial \lambda_c}{\partial i_b} & \frac{\partial \lambda_c}{\partial i_c} \end{bmatrix} = \begin{bmatrix} L^*_{aa}(i_{abc}, \theta) & L^*_{ab}(i_{abc}, \theta) & L^*_{ac}(i_{abc}, \theta) \\ L^*_{ba}(i_{abc}, \theta) & L^*_{bb}(i_{abc}, \theta) & L^*_{bc}(i_{abc}, \theta) \\ L^*_{ca}(i_{abc}, \theta) & L^*_{cb}(i_{abc}, \theta) & L^*_{cc}(i_{abc}, \theta) \end{bmatrix}$$

is the nonlinear inductance matrix which is also a composite function of the stator currents and rotor position.

B. Nonlinear Inductance Function

As described above, the inductance of the stator winding is a function of both the stator currents and the rotor position, which are linear independent [9]. For a fixed rotor position, the inductance curve can be expressed as a multinomial

$$L(i) = l_0 + l_1 i^1 + l_1 i^2 + \cdots + l_m i^m \tag{5}$$

where l_0, l_1, $l_2 \ldots$ l_m are the inductance coefficients.

On the other hand, for a constant stator current, the inductance is a periodic function of the rotor position [8]. It can be expressed as the sum of a series of sinusoidal harmonics by using Fourier Series as

$$L(\theta) = a_0 + \sum_{n=1}^{\infty} (a_n \cos(n\theta) + b_n \sin(n\theta)) \tag{6}$$

Then a composite function of both the current and rotor position can be defined to express the inductance as

$$L(i, \theta) = I(i) \cdot A \cdot C(\theta) \tag{7}$$

where $I(i) = [1 \quad i^1 \quad i^2 \quad \cdots \quad i^m]$;

$C(\theta) = [1 \quad \sin(\theta) \quad \cos(\theta) \quad \cdots \quad \sin(n\theta) \quad \cos(n\theta)]^T$; and

$A = \begin{bmatrix} a_{0,0} & a_{0,1} & \cdots & a_{0,2n} \\ a_{1,0} & a_{1,1} & \cdots & a_{1,2n} \\ \vdots & \vdots & \ddots & \vdots \\ a_{m,0} & a_{m,1} & \cdots & a_{m,2n} \end{bmatrix}$ is an identifiable parameter matrix.

C. Inductance Parameter Identification

The magnetization curve is usually expressed by using a fifth or seventh order multinomial. In order to fit a seventh order saturation curve, *m* is set to 6 in (5) and (7).

On the other hand, for the periodic inductance variation with respect to rotor position, the order of Fourier component vector $C(\theta)$ is chosen based on the harmonics weights. A series of inductance are recorded with a resolution of 6 electrical degrees when the stator currents are fixed at several different levels from 0 to 6.5A, respectively, while the magnetic circuit is fully saturated at 6.5A. The nameplate parameters of the tested SPMSM are shown in Table I.

TABLE I. PARAMETERS OF TESTED SPMSM

Model	IFT 6071-6AC21-2-Z
Number of Poles	6
Rated Power	1000 W
Rated Voltage	128 V
Rated Current	6.5 A
Rated Speed	2000 rev/min
Rated Torque	4.5 Nm (4.8?)

It is found that the harmonics of the inductance will converge in the first 11 components based on the FFT of the inductances at different currents. In order to regress the inductance-position curve accurately, *n* is set to be 12 in (7).

Therefore, the dimensions of matrix A are set to 7*25, by setting $m=6$ and $n=12$ to acquire an accurate enough surface regression.

The inductances are small and periodically fluctuant function. To obtain better regression results, the Least Relative Residual Sum of Square (LRRSS) method is employed. For the objective function $L(i,\theta)$, the relative residual sum of square is defined as

$$E_{re}(A)=\sum_{i=0}^{6}\sum_{\theta=0}^{2\pi}[\frac{I(i)\cdot A\cdot C(\theta)-L_{test}(i,\theta)}{L_{test}(i,\theta)}]^2 \qquad (8)$$

where $L_{test}(i,\theta)$ is the tested inductance value.

The same regression method is applied to the self- and mutual-inductance coefficients identification. Then a nonlinear inductance model is built up for this three-phase machine. An accurate inductance matrix can be calculated for given stator currents and rotor position. This model incorporates both the structural and saturation saliencies of the machine.

D. Nonlinear Machine Model for Numerical Simulation

Based on the nonlinear self- and mutual-inductance functions, an SPMSM model is built up in SIMULINK to numerically simulate the performance.

Fig. 1 shows the comparison between the simulated and measured self-inductance of phase *a* at 0A and 6A current offsets, where ±0.5% error bands are added. It can be found that the relative errors of inductances are very small.

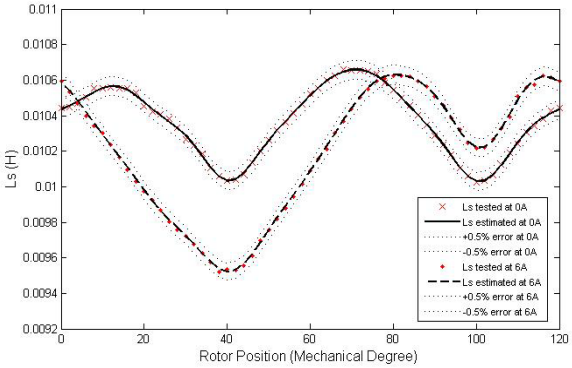

Figure 1. Measured and estimated self-inductance at different current offsets.

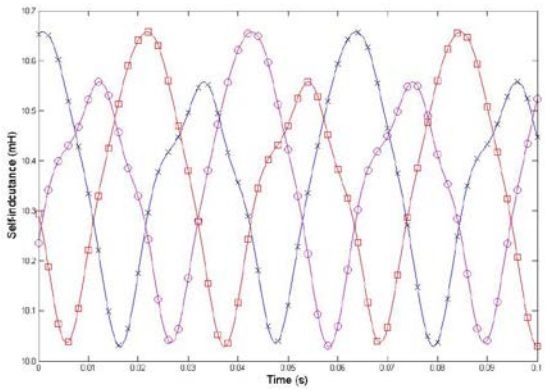

Figure 2. Unsaturated three-phase self-inductance curves at no-load.

Three-phase sinusoidal stator currents are input to the model with the synchronous rotor position. When the motor operates at no-load or a light load, the current amplitude is small and there is no saturation in the stator core. The inductance curves are unsaturated as shown in Fig. 2. It can also be found that the structural saliency is very small and the period of phase self-inductance can be assumed to be π.

Then, a larger current vector is input to the stator windings at which the stator core will be fully saturated. Based on the experiment results of inductance tests, the currents are set at 6.5A and the saturated inductance curves are shown in Fig. 3. It can be found that the saturation effect changes the inductance profile and the period of phase self-inductance is 2π, in which the rotor polarity is involved.

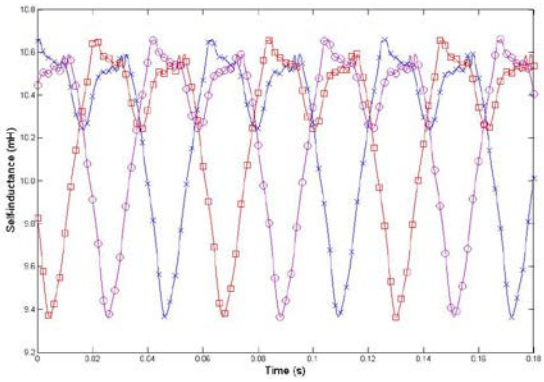

Figure 3. Saturated three-phase self-inductance curves at 6.5A stator current.

III. INITIAL ROTOR POSITION DETECTION

A. Rotor Vibration Limitation

Like the pulse injection method, most of the reported initial rotor position detection methods are based on electrical excitation, in which an electrical voltage or current signal is applied to the stator, the excited currents are observed and the rotor position is estimated. On the other hand, the injected signal should be carefully chosen in order to keep the rotor stationary. In the traditional development process, the experimental trial and error method has to be applied to test the rotor vibration and to determine the injected pulse width and magnitude. In this paper, mathematic analysis of the injection process is carried out and the rotor vibration is expressed by using the injected signal with the machine model parameters.

In the pulse injection method, a series of DC voltage pulse are injected into the stator winding to identify the rotor position. By assuming the electrical angle between the rotor d-axis and the injected voltage vector is δ, the d- and q-axis voltages can be expressed as

$$\begin{cases} v_d = V_{in}\cos(\delta+\omega t) \\ v_q = V_{in}\sin(\delta+\omega t) \end{cases} \qquad (9)$$

where V_{in} is the injected voltage magnitude.

In the rotor initial position detection algorithm, the rotor position is assumed to be constant or vary in a very small range. The voltages projected on the d- and q-axis are then considered as constant and the back-emf induced can be

ignored. The electrical process inside the stator windings can be expressed in the d-q reference frame as

$$\begin{cases} v_d = Ri_d + L_d \dfrac{di_d}{dt} \\ v_q = Ri_q + L_q \dfrac{di_q}{dt} \end{cases} \quad (10)$$

$$T_{em} = \frac{p}{2} \cdot \lambda_m \cdot i_q$$

The mechanical process inside the machine can be expressed as

$$T_{em} = T_{load} + F \cdot \frac{d\theta}{dt} + J \cdot \frac{d^2\theta}{dt^2} \quad (11)$$

Once the pulse injection method is applied to detect the rotor initial position, the resultant rotor speed is small enough so that the friction could be neglected. On the other hand, the angle vibrating limitation calculated under the zero friction assumption could easily satisfy the real system, where the unavoidable friction will further limit the rotor movement.

By substitute (9) and (10) to (11), we can solve the rotor mechanical angle as

$$\theta = \delta \cdot \frac{2}{p} + \frac{p}{2} \cdot \frac{\lambda_m \cdot V_{in} \sin(\delta)}{J \cdot R} \left[\frac{t^2}{2} + \left(\frac{L_q}{R} \right)^2 \left(1 - e^{-\frac{R}{L_q} t} \right) - \frac{L_q}{R} \cdot t \right] \quad (12)$$

For any initial rotor angle δ, the rotor angle vibration under the DC injected voltage pulse is

$$\Delta\theta = \pm \frac{p}{2} \cdot \frac{\lambda_m \cdot V_{in}}{J \cdot R} \left[\frac{\Delta t^2}{2} + \left(\frac{L_q}{R} \right)^2 \left(1 - e^{-\frac{R}{L_q} \Delta t} \right) - \frac{L_q}{R} \cdot \Delta t \right] \quad (13)$$

where Δt is the injected pulse width.

B. DC Pulse Injection

In the DC pulse injection method, a positive or a negative voltage pulse is injected to the stator phase windings, *a*, *b* and *c*, respectively, with a limited pulse width. A DC current will be generated in the injected phase and the peak value of the current will be recorded. To bring down the excited current and prevent the rotor from moving, an opposite voltage pulse will be added to follow each injected signal. An example of the injected voltage and excited current waveforms are illustrated in Fig. 4.

All the injected voltage pulses are chosen based on (13) and the rotor vibration area is limited. When a low voltage pulse (50V, Δt =0.0004s) is injected, the rotor movement is limited within ±0.08 electrical degree. When a high voltage pulse (300V, Δt =0.0004s) is injected, the rotor movement is limited within ±0.5 electrical degree. Fig. 5 shows the maximum rotor vibrating angle under different voltage pulses injection.

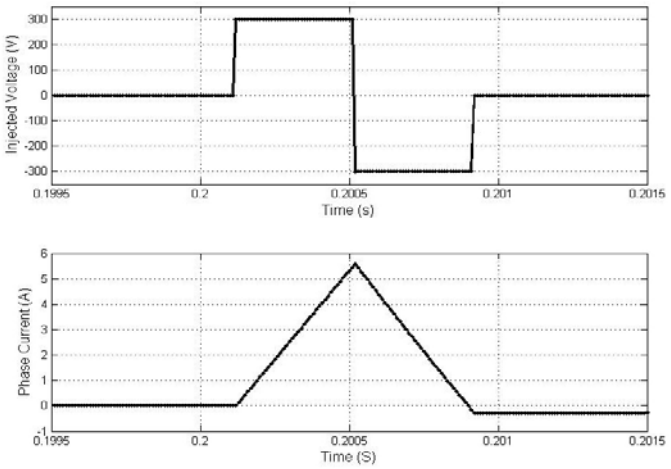

Figure 4. Injected DC voltage pulse and excited phase current.

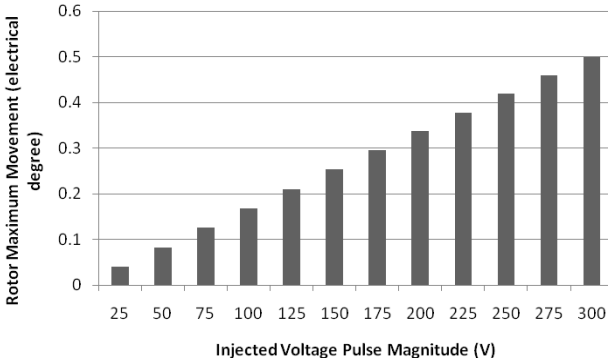

Figure 5. Maximum rotor movement angle under different voltage pulses injection, Δt =0.0004s.

The modeled machine has six poles and it can be calculated from Fig. 5 that the maximum rotor vibrating angle is smaller than 0.2 mechanical degree. This value is acceptable for the numerical simulation to assume the rotor is kept at standstill. As discussed above, this angle value will be further reduced in the real time experiment, where the shaft friction does exist.

For a limited voltage pulse width, the rotor movement is usually very small and the peak current value of the injected phase is inversely proportional to the phase self-inductance [8], which is a periodic function of the rotor angle as shown in Figs. 2 and 3.

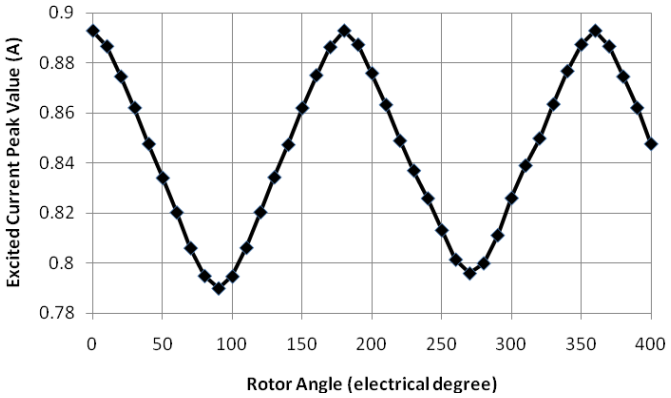

Figure 6. Excited peak current under a low voltage pulse injection.

Fig. 6 shows the peak current value against the initial rotor angle when a 50V voltage pulse is injected into the stator winding. It can be find out that the current peak value will reach the maximum value twice in one electrical cycle, where the rotor axis aligns with the injected stator phase.

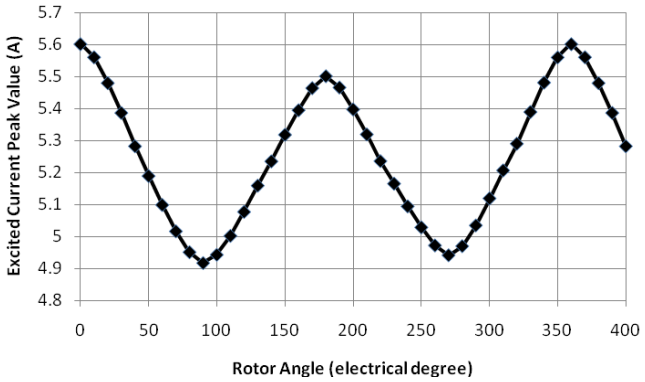

Figure 7. Excited peak current under a high voltage pulse injection.

Then a higher voltage pulse is injected and the magnitude of voltage pulse is set to 300V. It can be seen from Fig. 7 that the excited current peak value is still a function of the rotor angle but the two maximum current values are no longer equal, because the stator core is now saturated and the inductance values are not equal when the N pole or the S pole aligns with the excited stator phase.

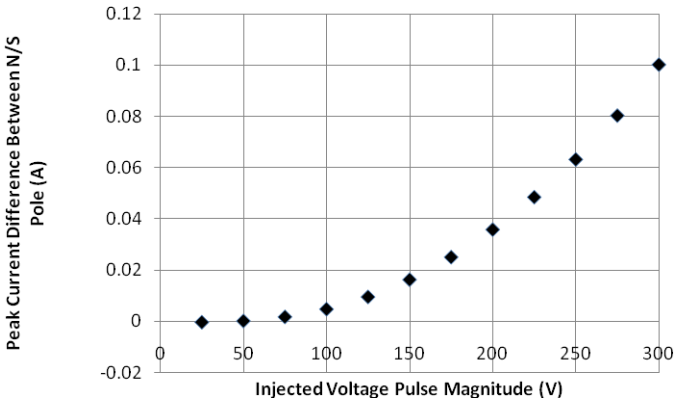

Figure 8. N/S pole current difference under different voltage pulses.

Fig. 8 shows the peak current difference when the N- or S-pole aligns with the under-injection stator phase. Under the low voltage pulse excitation, the generated current is small and the stator core is not saturated or not highly saturated. The peak currents under N- and S-pole are nearly equal. When the injected voltage magnitude is increased to a higher value, which will induce a bigger current in the stator phase, the stator core will be more saturated and the peak current difference under N- or S-pole will increase to a higher level as shown in Fig. 8. The relationship between the injected voltage and the current difference is not linear because of the nonlinear inductance model. The high level current difference could be obtained more easily in the real time experiment and it is useful for identifying the rotor magnet polarity.

C. Initial Rotor Position Detection

Based on the DC pulse injection analysis above, the three-phase peak current profile is close to a second order sinusoidal function against the rotor electrical angle. In order to determine the initial rotor position, positive and negative high magnitude voltage pulses are injected into the stator windings. As shown in Fig. 9, the three phase current responses are balanced well and the saturation caused by the rotor magnets can also be observed.

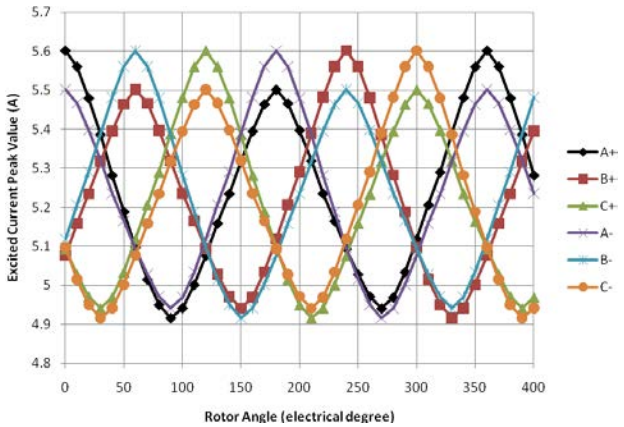

Figure 9. Three-phase excited peak current profile under high voltage pulses.

For an unknown rotor position, the response peak currents are marked as I_{A+}, I_{A-}, I_{B+}, I_{B-}, I_{C+} and I_{C-}, where A, B, C represent the three stator phases and +/- represent the injected positive or negative voltage pulse. The current values can be approximately expressed as balanced three-phase sinusoidal waves.

As shown in Fig. 9, the electrical cycle is divided to six sectors and each sector can be addressed by tracking the maximum current peak value. Then, the angle offset inside the sector can be calculated based on the other two phase current peaks. The detection procedure is described in Fig. 10.

In order to minimize the rotor movement, the low voltage pulses are applied firstly. The two biggest current peak values in one phase, under positive and negative excitations, are used to determine the rotor axis position. Then high magnitude positive and negative voltage pulses are applied to that phase, which is close to the rotor d-axis. According to Fig. 8, the peak current difference under the positive and negative pulses will be observable to detect the rotor polarity. In this procedure, the high voltage pulses are usually injected to the phase close to the d-axis so that the rotor vibration is minimized.

After obtaining the rotor N pole position, the rotor angle sector can be determined as shown in Fig. 9. The angle offset is calculated based on the other two current peak values. For example, if the rotor axis is detected near phase A, then the current peak values in phases B and C will be used to calculate the angle offset value. The values recorded under low and medium voltage pulse excitations are used to calculate and compensate the angle offset value. According to Fig. 6, the unsaturated current response is closer to a second order sinusoid.

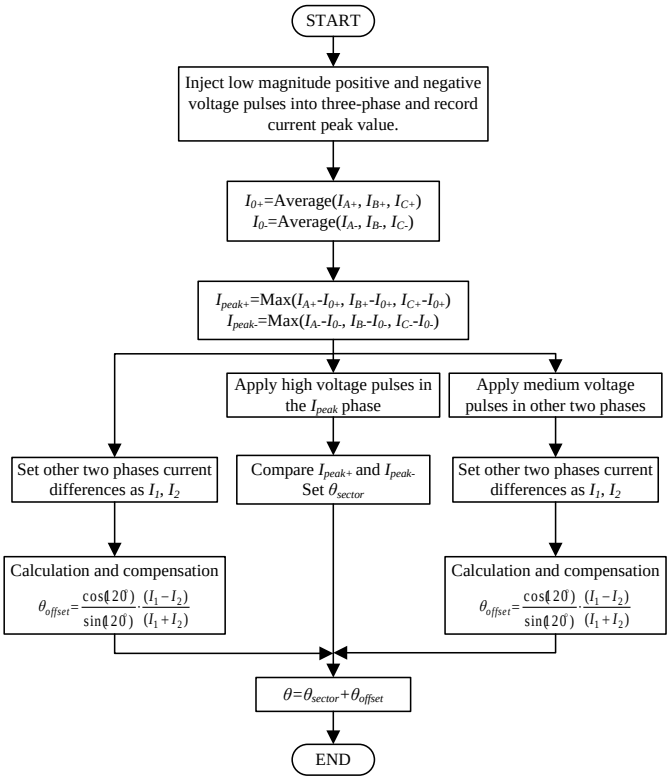

Figure 10. Rotor position estimation procedure.

IV. Simulation Performance

The proposed method is applied to the nonlinear machine model in SIMULINK. The initial rotor position is set to several values and simulation is conducted. Fig. 11 shows the rotor angle detection results at different rotor positions.

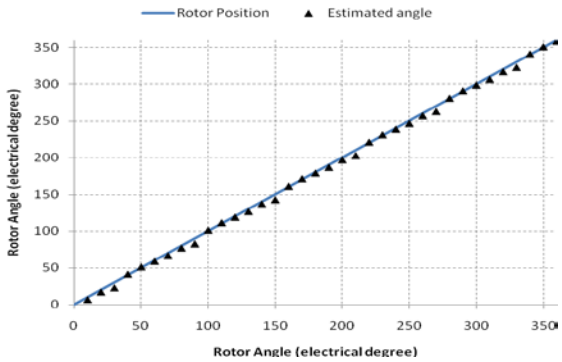

Figure 11. Estimated initial rotor position.

It can be found out that the estimated initial rotor angle is close to the real rotor position and the error of the estimation is limited within ±7 electrical degrees, or ±2.3 mechanical degrees. When the rotor position is away from the sector center, the error becomes bigger, because the three-phase peak current response is not exactly a second sinusoid of rotor position. At the same time, the rotor vibration is further reduced to ±0.3 (unit), smaller than that in Fig. 5, because only the low and medium voltage pulses are injected in all the three phases and the high voltage pulses are injected around d-axis so the generated instantaneous torque is small.

V. Conclusion

The nonlinearity of the PMSM machine model is mainly caused by the saturable inductances of stator windings. In this paper, a composite function is designed to express the inductance as the function of both the stator current and the rotor position which are de-coupled. A nonlinear model of SPMSM is setup based on this function. With the identified coefficients, the new SPMSM model is built up in MATLAB/SIMULINK. The unsaturated and the saturated inductance curves are simulated. Based on this new comprehensive model, simulation of novel drive methods will be possible, avoiding the experimental trial and error process, reducing the develop cycle time and saving research costs.

The rotor vibration analysis is carried out based on DC pulse injection, which is an effective initial rotor position detection scheme. The rotor maximum vibrating angle is expressed as a function of the injected voltage signal width and magnitude. The injected voltage signal is then specified to keep the rotor at standstill.

Based on the injected voltage pulses and the nonlinear machine model, numerical simulation of the current response is carried out, in which the saturation saliency is detected and used to identify the rotor polarity. The excited peak currents are recorded to calculate the rotor position by the estimation procedure provided. The simulation is taken at several different initial rotor positions and the result shows that the estimation error is small, showing that the proposed method can be applied to detect the initial rotor position and magnet polarity.

References

[1] Y. Yamamoto, Y. Yoshida, and T. Ashikaga, “Sensorless control of PM motor using full order flux observer,”, IEEE Transactions on Industrial Applications, vol. 124, no. 8, pp. 743–749, Aug. 2004.

[2] M. E. Haque, L. Zhong, and M. F. Rahman, “A sensorless initial rotor position estimation scheme for a direct torque controlled interior permanent magnet synchronous motor drive,” IEEE Transactions on Power Electronics, vol. 18, no. 6, pp. 1376–1383, Nov. 2003.

[3] E. Robeischl, M. Schroedl, and M. Krammer, “Position-sensorless biaxial position control with industrial PM motor drives based on INFORM-method and back EMF model,” in Proceedings of the IEEE-IES Annual Conference, 5-8 Nov. 2002, vol. 1, pp. 668– 67.

[4] S. Kondo, A. Takahashi, and T. Nishida, “Armature current locus-based estimation method of rotor position of permanent magnet synchronous motor without mechanical sensor,” in Proceedings of IEEE-IAS Annual Meeting, 1995, vol. 1, pp. 55–60.

[5] Y. Yan, J. G. Zhu, Y. G. Guo, and H. Lu, “Modeling and simulation of direct torque controlled PMSM drive system incorporating structural and saturation saliencies,” in Proceedings of the 41st IEEE IAS Annual Meeting, Tampa, FL, Oct. 2006, pp. 76-83.

[6] P. B. Schmidt, “Method and apparatus for rotor angle detection,” U.S. Patent 6 172 498, Jan. 9, 2001.

[7] Y. Yan, J. G. Zhu and Y. G. Guo, “A direct torque controlled surface mounted PMSM drive with initial rotor position estimation based on structural and saturation saliencies,” in Proceedings of the 41st IEEE IAS Annual Meeting, New Orleans, LA, Sept. 2007, pp. 683-689.

[8] P. Cui, J. G. Zhu, Q. P. Ha, G. P. Hunter, and V. S. Ramsden, “Simulation of non-linear switched reluctance motor drive with PSIM,” in Proceedings of the 5th International Conference on Electrical Machines and Systems, vol. 1, Aug. 2001, pp. 1061-1064.